Supporting Information

Kuroki et al. 10.1073/pnas.1324105111

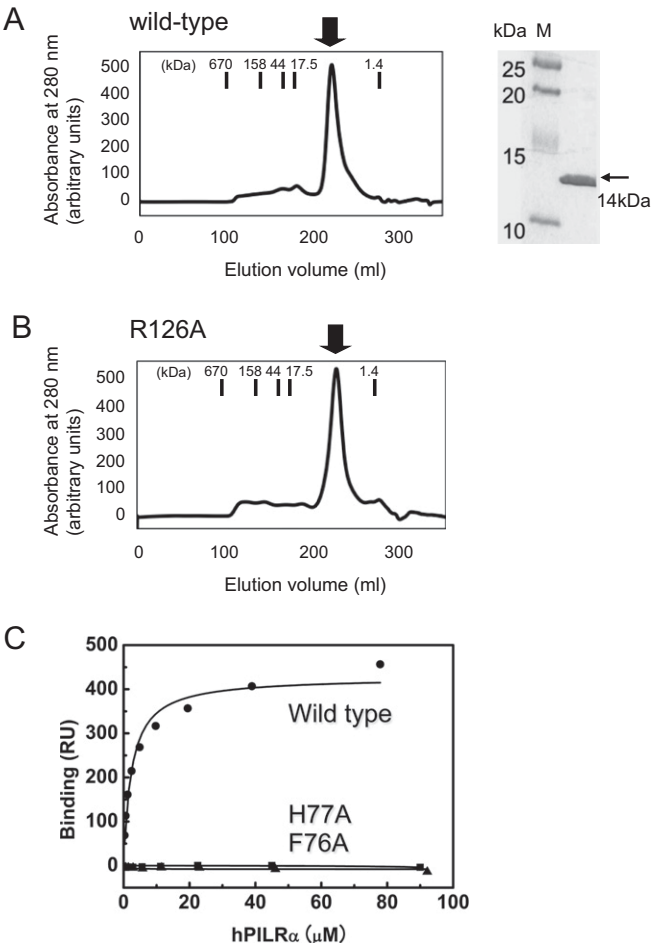

Fig. S1. Preparation and surface plasmon resonance (SPR) binding study of paired Ig-like type 2 receptor alpha (PILRα). (*A* and *B*) Gel filtration of wild-type (*A*) and mutant (*B*) refolded PILRα. The arrows indicate the peaks of the PILRα proteins, showing the mass of their monomeric form. SDS/PAGE also shows a single band in the wild-type PILRα, demonstrating a mass of 14 kDa consistent with the calculated molecular mass (*Right*). (*C*) Representative SPR binding studies with HSV glycoprotein B (gB) of wild-type PILRα (closed circles) and the H77A and F76A mutants (closed squares and triangles, respectively). Responses at serial concentrations of PILRα proteins were determined and fitted by the 1:1 Langmiur binding model. RU, resonance units.

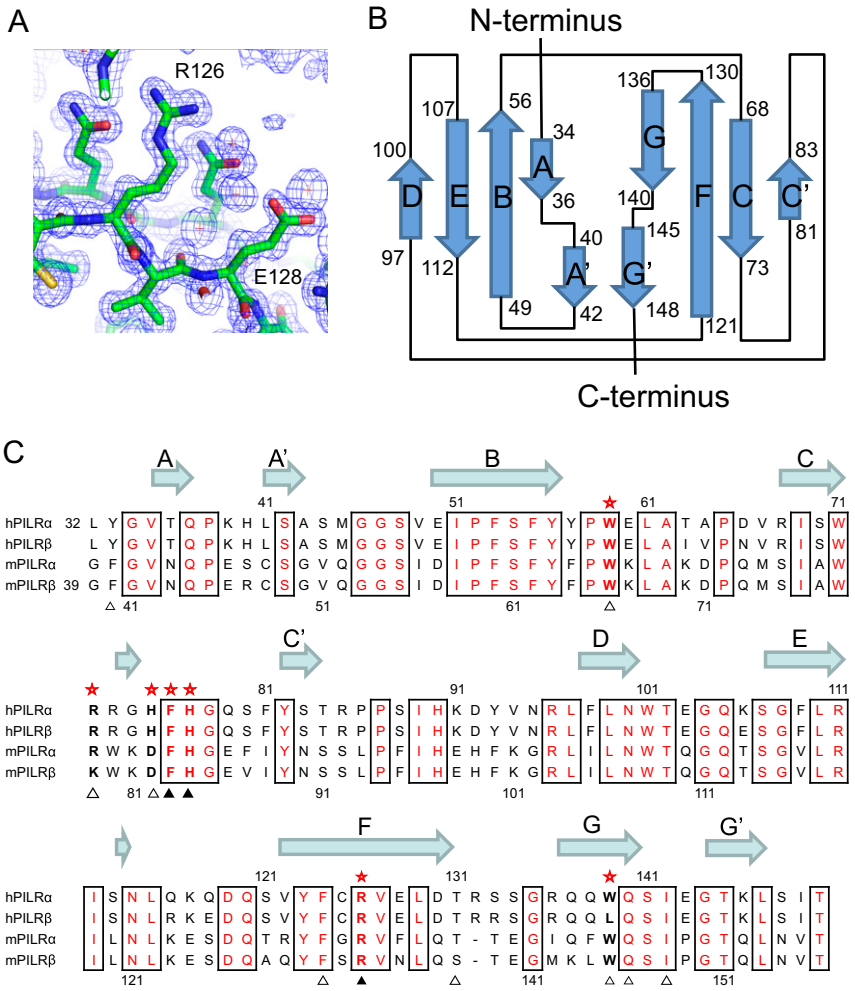

Fig. S2. Crystal structure of the free form, topology, and comparison of amino acid sequences in PILRα. (*A*) *2Fo-Fc* electron density map of the free form of PILRα (1.3 Å). (*B*) Topological diagram of the free form of wild-type PILRα. The β-strands (A to G) are shown in cyan arrows. (*C*) Alignment of the amino acid sequences of human PILRs with mouse PILRs. Boxes with red characters indicate the conserved amino acids. Numbers above and below the alignments indicate the amino acid numbers in human PILRα and mouse PILRβ, respectively. Stars above the alignments indicate amino acids whose mutations reduce the infectious activity. The open and closed triangles below the alignments indicate amino acids whose mutations reduced (open triangles) or lost (closed triangles) the binding activity to HSV-1 gB, as shown by SPR experiments.

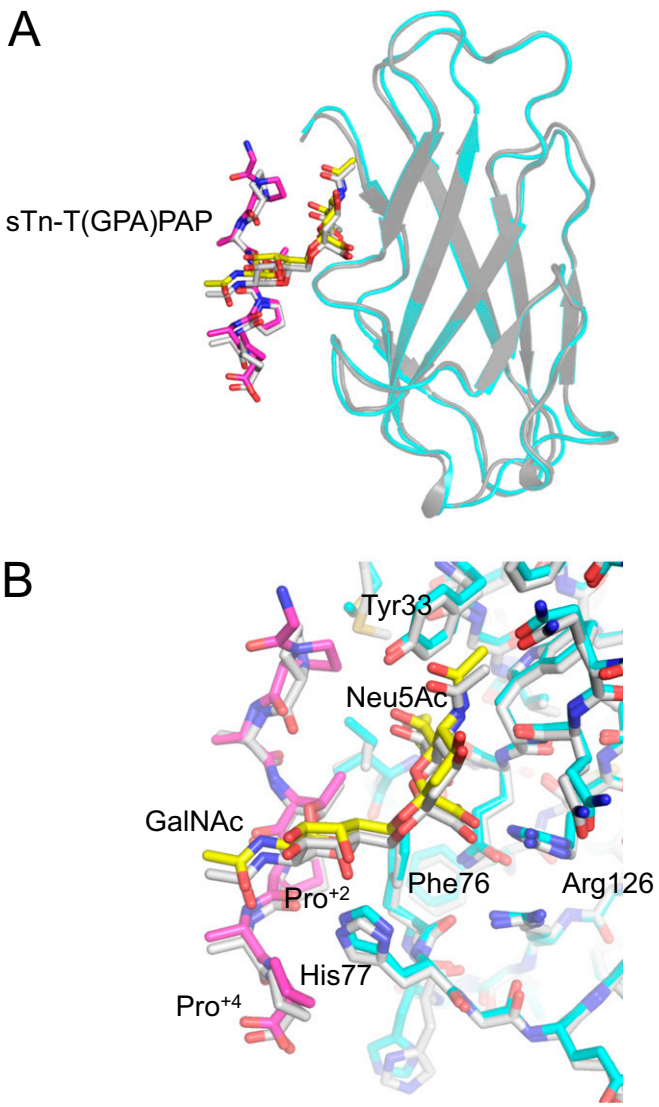

Fig. S3. Structural comparison of two PILRα-sugar T antigen (sTn) peptide complexes in the asymmetric unit. (*A*) Cartoon model showing the structure of PILRα–sTn peptide complex A (cyan) and B (gray). A stick model of bound sTn peptide [GPAT(sTn)PAP] in the A complex is shown (peptide region: magenta; glycan: yellow). The rmsd difference between these structures is 0.57 Å. (*B*) Detailed view of the interaction sites. These complexes are essentially the same, and therefore we focus on complex A in the main text.

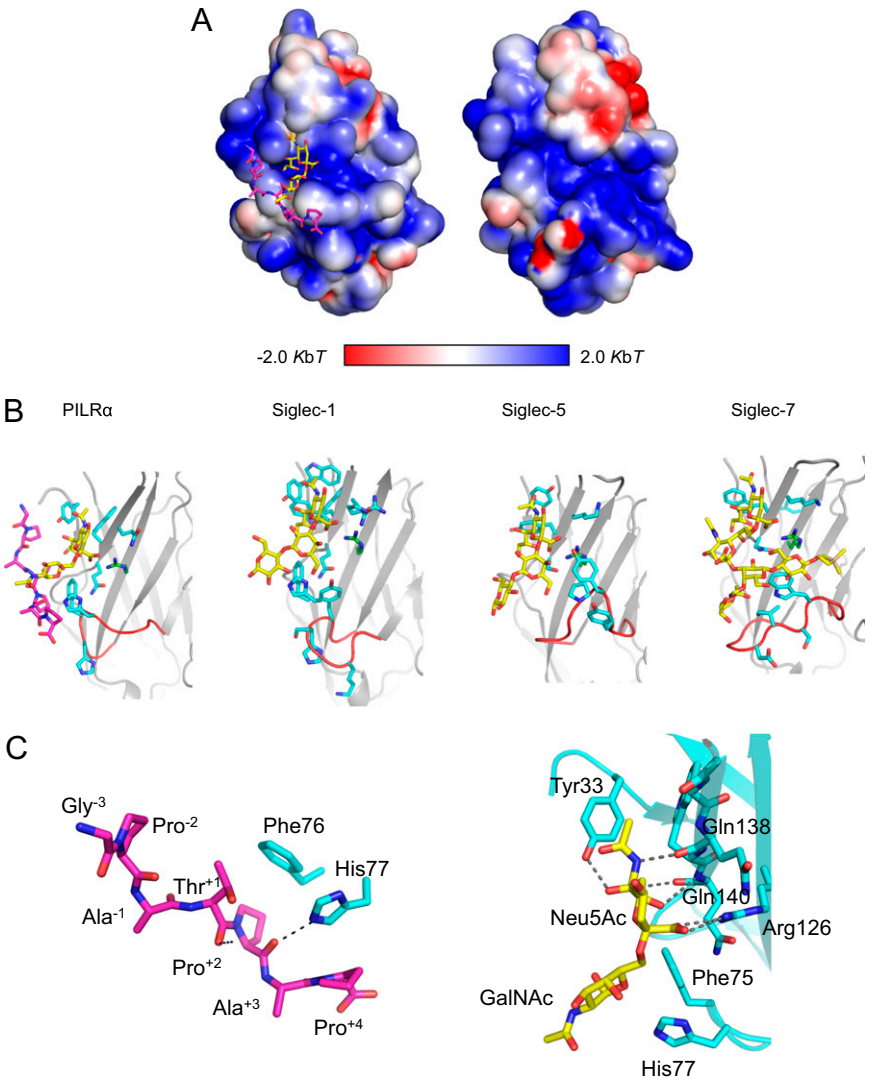

Fig. S4. (*A*) Representation of the surface potential of complex (*Left*) and free (*Right*) PILRα, with carbohydrate moieties shown as sticks. (*B*) Structural comparison of the sugar-recognition modes of PILRα (*Left*) and sialic acid-binding Ig-like lectin (Siglec) family members Siglec-1 (*Center Left*), -5 (*Center Right*), and -7 (*Right*). The CC′ loops with a part of the D strand are represented in red. The proteins are shown in cartoon style, and ligand sugars are shown as dark blue-based stick models. The green residues correspond to "essential R." (*C*) Detailed interaction of the peptide and sTn with PILRα.

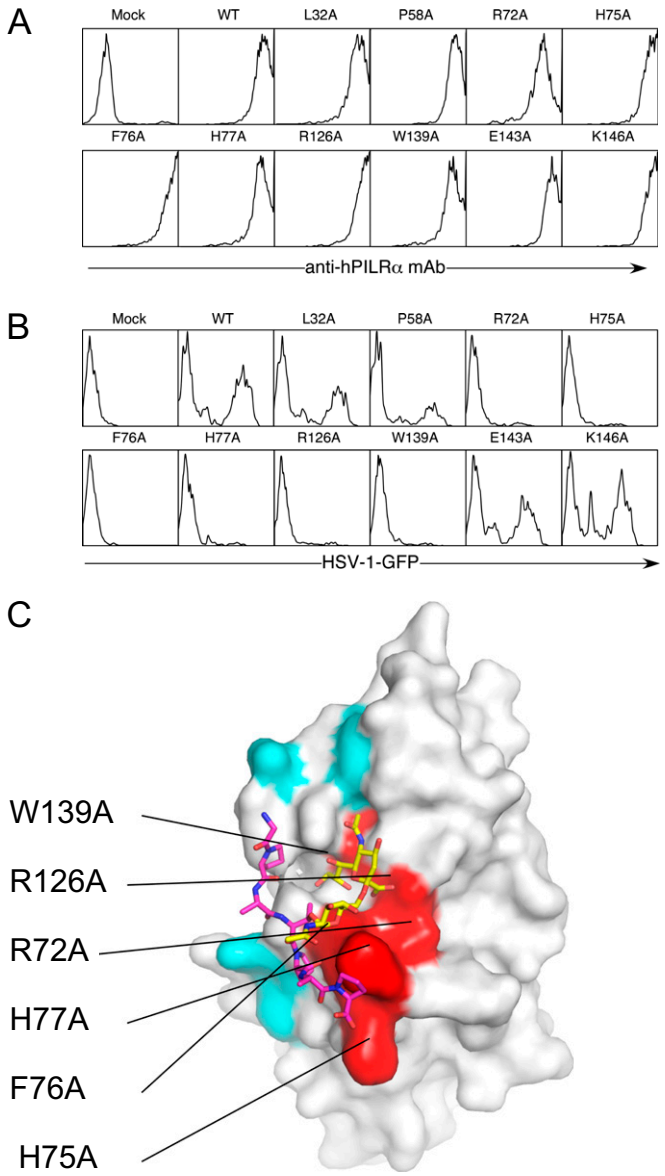

Fig. S5. Assays of PILRα-mediated infection. (*A*) HEK293 cells were transiently transfected with the pMx-IRES-DsRed expression vector containing wild-type PILRα or PILRα mutants. The transfected cells were stained by anti-human PILRα antibody (M4) and were analyzed by flow cytometry. The histograms represent the DsRed-gated population. (*B*) PILRα-ligand–negative CHO-K1 cells were transiently transfected with the pMx-IRES-DsRed expression vector containing wild-type PILRα or PILRα mutants. The transfected cells were infected with HSV-1-GFP. Dsred-positive cells expressing GFP were analyzed by flow cytometry. The histograms show fluorescence intensity measured in arbitrary units on a log scale (*x* axis) and relative cell number on a linear scale (*y* axis). (*C*) HSV-1 infectious activity in cells expressing wild-type or mutant PILRα protein. The significant residues in which mutations showed little infectious activity are mapped (red, Arg72, His75, Phe76, His77, Arg126, and Trp139). Cyan coloring indicates residues whose mutations did not affect infectious activity.

Table S1. Data collection and refinement statistics

Crystallographic parameters	PILRα–sTn peptide complex	Free form of PILRα
Data collection		
Space group	$C222_1$	$P2_12_12_1$
Cell dimensions		
a, *b*, *c*, Å	50.27, 155.80, 67.31	40.33, 44.94, 56.87
Resolution, Å*,†	20–2.30 (2.42–2.30)	20–1.3 (1.33–1.30)
R_{merge}†	0.168 (0.567)	0.058 (0.375)
$I/\sigma I$†	10.5 (3.1)	13.1 (4.1)
Completeness, %†	99.7 (99.7)	99.9 (99.8)
Redundancy†	6.9 (5.1)	7.0 (6.8)
Refinement		
Resolution, Å	20–2.30 (2.37–2.30)	20–1.3 (1.33–1.30)
No. of unique reflections	12,109	24,742
R_{work}/ R_{free}‡	0.231/0.299	0.144/0.177
No. atoms		
Protein	1,962	1,004
Ligand/ion	190	30
Water	162	93
B-factors, Å^2		
Protein	16.7	17.4
Ligand/ion	26.7	22.4
Water	19.3	25.7
Rmsd		
Bond lengths, Å	0.0064	0.012
Bond angles,°	1.23	1.47
Ramachandran plot§		
Most favored	230 (94.7%)	113 (95.8%)
Additional allowed	13 (5.3%)	5 (4.2%)
Disallowed	0 (0%)	0 (0%)

*One crystal was used.
†Highest-resolution shell is shown in parenthesis.
‡Of the total reflections, 5.0% were held aside for R_{free} throughout refinement.
§Analyzed by RAMPAGE (1).

1. Lovell SC, et al. (2003) Structure validation by Cα geometry: ϕ,ψ and Cβ deviation. *Proteins* 50(3):437–450.

Table S2. Intermolecular contacts (located within 4 Å) in PILRα-sTn peptide complex

Ligand. gB	PILRα	Distance, Å
van der Waals interaction (intermolecular)		
Pro^{-2} Cδ	Met31 Cε	3.4
Pro^{-2} Cβ	Met31 Cε	3.4
Pro^{-2} Cγ	Met31 Cε	3.3
Pro^{-2} Cδ	Tyr33 OH	3.4
Pro^{-2} Cγ	Tyr33 OH	3.9
Pro^{-2} Cβ	Ile142 Cδ1	3.8
Pro^{-2} Cγ	Ile142 Cδ1	3.9
Ala^{-1} O	Ile142 Cδ1	3.8
Ala^{-1} O	Ile142 Cγ2	3.9
Pro^{+2} Cδ	Phe76 Cγ	3.9
Pro^{+2} Cδ	Phe76 Cδ2	3.8
Pro^{+2} Cγ	Phe76 Cβ	3.4
Pro^{+2} Cγ	Phe76 Cγ	3.4
Pro^{+2} Cγ	Phe76 Cδ1	4.0
Pro^{+2} Cγ	Phe76 Cδ2	3.8
Pro^{+2} C	His77 Nε2	3.8
Pro^{+2} O	Phe76 Cδ2	3.4
Pro^{+4} N	Phe76 Nε2	3.9
Pro^{+4} N	Phe76 Nδ2	3.9
Pro^{+4} Cα	Phe76 Nδ2	3.7
Pro^{+4} Cβ	Phe76 Nδ2	4.0
Neu5Ac C10	Tyr33 Cε2	4.0
Neu5Ac C10	Tyr33 Cζ	3.6
Neu5Ac C11	Tyr33 Cδ2	4.0
Neu5Ac C11	Tyr33 Cε2	3.7
Neu5Ac C11	Tyr33 Cζ	3.8
Neu5Ac C11	Trp139 CH2	3.8
Neu5Ac C11	Gln138 O	3.8
Neu5Ac C11	Gln137 Oε1	3.2
Neu5Ac C7	Trp139 Cβ	3.8
Neu5Ac C7	Tyr33 Cε1	3.7
Neu5Ac O7	Tyr33 Cε1	3.7
Neu5Ac O7	Tyr33 Cζ	3.6
Neu5Ac O8	Trp139 Cα	3.7
Neu5Ac O8	Trp139 Cβ	3.9
Neu5Ac O8	Gln137 Oγ	3.9
Neu5Ac O8	Phe76 Cζ	3.8
Neu5Ac C9	Gln140 O	3.4
Neu5Ac C9	Trp139 Cβ	3.6
Neu5Ac C9	Gln140 N	3.9
Neu5Ac C9	Tyr33 Cε1	3.5
Neu5Ac O9	Ile142 Cγ1	2.9
Neu5Ac O9	Ile142 Cδ1	3.2
GalNAc C1	His77 Nε2	4.0
GalNAc C1	His77 Cε1	4.0
GalNAc C6	His77 Cε1	4.0
GalNAc O5	Phe76 Cε1	4.0
GalNAc O5	His77 Cε1	3.1
Hydrogen bond (intermolecular)		
Pro^{+2} O	His77 Nε2	2.6
Neu5Ac O1α	Arg126 NH1	2.9
Neu5Ac O1β	Arg126 NH2	2.7
Neu5Ac N5	Gln138 O	2.7
Neu5Ac O7	Tyr33 OH	2.7
Neu5Ac O10	Tyr33 OH	3.1
Neu5Ac O8	Gln140 N	3.4
Neu5Ac O9	Gln140 O	3.1

Table S3. Binding affinities of wild-type and mutant PILRα proteins for HSV-1 gB, determined by SPR

Analyte	K_d, μM	Analyte	K_d, μM
WT	2.3 ± 0.1	V122A	2.3 ± 0.1
L32A	1.6 ± 0.1	F124A	44 ± 2.2
Y33A	13 ± 0.4	R126A	No binding
Y57A	6.0 ± 0.1	E128A	1.5 ± 0.1
P58A	2.3 ± 0.0	T131A	8.3 ± 0.3
W59A	7.7 ± 0.2	S134A	2.4 ± 0.2
R68A	2.3 ± 0.1	Q137A	4.1 ± 0.3
S70A	2.5 ± 0.2	Q138A	2.7 ± 0.3
R72A	178 ± 8.3	W139A	134 ± 5.0
H75A	29 ± 1.0	Q140A	40 ± 0.9
F76A	No binding	S141A	3.0 ± 0.2
H77A	No binding	I142A	23 ± 0.8
Q79A	2.6 ± 0.2	E143A	1.2 ± 0.0
S88A	2.8 ± 0.1	K146A	3.1 ± 0.0
Q105A	2.8 ± 0.1		

K_ds were determined by equilibrium-binding experiments using SPR. Representative examples are shown in Fig. S1.